

## Modulation of *Bacillus subtilis* Catabolite Repression by Transition State Regulatory Protein AbrB

SUSAN H. FISHER,<sup>1\*</sup> MARK A. STRAUCH,<sup>2</sup> MARIETTE R. ATKINSON,<sup>1</sup> AND LEWIS V. WRAY, JR.<sup>1</sup>

<sup>1</sup>Department of Microbiology, Boston University School of Medicine, Boston, Massachusetts 02118,  
and Division of Cellular Biology, Department of Molecular and Experimental Medicine, Research Institute  
of Scripps Clinic, La Jolla, California 92037<sup>2</sup>

Received 4 October 1993/Accepted 26 January 1994

The first enzyme of the *Bacillus subtilis* histidine-degradative (*hut*) pathway, histidase, was expressed at higher levels during the onset of the stationary growth phase in nutrient sporulation medium in early-blocked sporulation mutants (*spo0A*) than in wild-type strains. Histidase expression was also elevated in *spo0A* mutant cultures compared with wild-type cultures during the logarithmic growth phase in minimal medium containing slowly metabolized carbon sources. Histidase expression was not derepressed in *spo0A abrB* mutant cultures under these growth conditions, suggesting that the AbrB protein is responsible for the derepression of histidase synthesis seen in *spo0A* mutant cultures. *spo0A* mutants contain higher levels of the AbrB protein than do wild-type strains because the Spo0A protein represses AbrB expression. A direct correlation between the levels of *abrB* transcription and histidase expression was found in *spo0A* mutant cultures. The *hutO*<sub>CR2</sub> operator, which is required for wild-type regulation of *hut* expression by catabolite repression, was also required for AbrB-dependent derepression of *hut* expression in *spo0A* mutants. Purified AbrB protein bound to the *hutO*<sub>CR2</sub> operator in vitro, suggesting that AbrB protein alters *hut* expression by competing with the *hut* catabolite repressor protein for binding to the *hutO*<sub>CR2</sub> site. During the logarithmic growth phase in media containing slowly metabolized carbon sources, the expression of several other enzymes subject to catabolite repression was elevated in *spo0A* mutants but not in *spo0A abrB* mutants. This suggests that the AbrB protein acts as a global modulator of catabolite repression during carbon-limited growth.

As *Bacillus subtilis* cultures enter the stationary growth phase in nutrient sporulation medium, the supply of rapidly metabolizable compounds is depleted. This results in global changes in gene expression which allow cells to adapt to growth and survival in the altered nutritional environment. Catabolic enzymes whose expression is derepressed under these growth conditions include proteases (36, 39); the arginine-, proline-, and histidine-degradative enzymes (3, 11);  $\alpha$ -amylase (36); and the enzymes of the citric acid cycle (12, 29, 36). In addition, transport of amino acids and dipeptides is increased (3, 4, 10, 21), peptide antibiotics are produced (36, 39), and cells become motile and can develop competence (36, 39). Ultimately, if growth does not resume, sporulation can be initiated.

Multiple proteins, including AbrB, ComA, Hpr, and SinR, are responsible for the regulation of gene expression seen during this transition period (39). The AbrB protein is involved in regulation of the expression of many post-exponential-phase functions, including proteases, motility, competence, dipeptide transport, antibiotic production, and Hpr expression (17, 38). Transcription of the *abrB* gene is repressed by its own product, AbrB, and by the Spo0A protein (31, 40). During the transition to the stationary growth phase in nutrient broth sporulation medium, the Spo0A protein is phosphorylated by a phosphorelay system (7). Since Spo0A~P has a higher affinity for the *abrB* promoter region than does the Spo0A protein, *abrB* transcription is repressed and AbrB levels decrease (38, 40).

Histidine degradation in *B. subtilis* supplies the cells with both ammonium (NH<sub>4</sub><sup>+</sup>) and L-glutamate (9). The genes that encode the histidine-degradative enzymes (*hut*) are organized

as a multicistronic operon (see Fig. 2; 9, 28). The first open reading frame in the *hut* operon, *hutP*, encodes a positive regulatory protein required for *hut* operon expression, while the second open reading frame, *hutH*, encodes the first enzyme in the histidine-degradative pathway, histidase (9, 28). A nucleotide sequence which can form a stem-loop structure is located between the *hutP* and *hutH* genes.

Expression of the *hut* operon during the logarithmic growth phase is induced by histidine and regulated in response to amino acid and carbon availability (2, 9). The histidine-dependent induction of *hut* operon expression has been proposed to be mediated by transcription antitermination at the putative stem-loop structure (28). During the exponential growth phase in nutrient sporulation medium, *hut* expression is repressed because of inhibition of transport of the *hut* inducer, histidine, by amino acids (3). Catabolite repression of *hut* expression is mediated at two *cis*-acting sites (27, 45). The *hutO*<sub>CR1</sub> site lies immediately downstream of the *hut* promoter and only weakly regulates *hut* expression. The *hutO*<sub>CR2</sub> site is located within the *hutP* gene, over 200 nucleotides downstream of the *hut* transcriptional initiation site, and is required for wild-type regulation of *hut* expression by catabolite repression. The nucleotide sequence of the *hutO*<sub>CR2</sub> site has strong similarity to the consensus sequence proposed for *B. subtilis* catabolite repression operators (44, 45). Since mutations in the *hutO*<sub>CR2</sub> site result in high levels of *hut* expression in glucose-grown cultures, catabolite repression of *hut* expression is most likely mediated by a negative regulatory system (45).

Altered expression of enzymes subject to catabolite repression in early-blocked sporulation (*spo*) mutants has been previously reported (5, 6). In this study, we found that elevated synthesis of *hut* and other enzymes seen in *spo0A* mutant cultures during the mid-exponential growth phase results from increased levels of AbrB. Interestingly, the AbrB protein

\* Corresponding author. Mailing address: Department of Microbiology, Boston University School of Medicine, 80 East Concord St., Boston, MA 02118. Fax: (617) 638-4286. Electronic mail address: shfisher@acs.bu.edu.

TABLE 1. *B. subtilis* strains used in this study

| Strain         | Description <sup>a</sup>   | Reference, source, or derivation             |
|----------------|--|--|
| JH642          | <i>trpC2 phe-1</i>   | J. Hoch                                      |
| JH12586        | $\Delta$ <i>abrB::cat trpC2 phe-1</i>  | J. Hoch, A. L. Sonenshein; 31                |
| SF513          | $\Delta$ <i>abrB::cat trpC2 phe-1</i>  | JH642 $\times$ JH12586 DNA                   |
| IS708          | $\Delta$ <i>hpr::cat leuA8 metB5 hisA1</i>   | I. Smith, A. Grossman; 30                    |
| JH642abrB::neo | <i>abrB::neo trpC2 phe-1</i>   | T. Tanaka, P. Zuber                          |
| JH12575        | <i>abrB::Tn917 trpC2 phe-1</i>   | J. Hoch; 31                                  |
| JH12663        | <i>abrB4 trpC2 phe-1</i>   | J. Hoch                                      |
| JH646          | <i>spo0A12 trpC2 phe-1</i>   | J. Hoch, M. Perego                           |
| JH703          | <i>spo0A12 trpC2 phe-1</i>   | J. Hoch                                      |
| SF511          | <i>spo0A12 <math>\Delta</math>abrB::cat trpC2 phe-1</i>  | JH642 $\times$ JH646 and SF513 DNAs          |
| SF514          | <i>spo0A12 <math>\Delta</math>abrB::neo trpC2 phe-1</i>  | JH642 $\times$ JH646 and JH642abrB::neo DNAs |
| SF515          | <i>spo0A12 <math>\Delta</math>hpr::cat trpC2 phe-1</i>   | JH642 $\times$ JH646 and IS708 DNAs          |
| JH646MS        | <i>spo0A12 <math>\Delta</math>abrB15 trpC2 phe-1</i>   | J. Hoch; 42                                  |
| R15-8          | <i>spo0A12 <math>\Delta</math>abrB20 trpC2 phe-1</i>   | J. Hoch; 42                                  |
| R15-9          | <i>spo0A12 <math>\Delta</math>abrB21 trpC2 phe-1</i>   | J. Hoch; 42                                  |
| R15-12         | <i>spo0A12 <math>\Delta</math>abrB22 trpC2 phe-1</i>   | J. Hoch; 42                                  |
| R15-13         | <i>spo0A12 <math>\Delta</math>abrB23 trpC2 phe-1</i>   | J. Hoch; 42                                  |
| JH703abrB1     | <i>spo0A12 <math>\Delta</math>204 <math>\Delta</math>abrB1 trpC2 phe-1</i>   | J. Hoch; 42                                  |
| JH703abrB2     | <i>spo0A12 <math>\Delta</math>204 <math>\Delta</math>abrB2 trpC2 phe-1</i>   | J. Hoch; 42                                  |
| JH703abrB3     | <i>spo0A12 <math>\Delta</math>204 <math>\Delta</math>abrB3 trpC2 phe-1</i>   | J. Hoch; 42                                  |
| JH703abrB4     | <i>spo0A12 <math>\Delta</math>204 <math>\Delta</math>abrB4 trpC2 phe-1</i>   | J. Hoch, M. Perego; 42                       |
| JH703abrB5     | <i>spo0A12 <math>\Delta</math>204 <math>\Delta</math>abrB5 trpC2 phe-1</i>   | J. Hoch; 42                                  |
| JH703abrB6     | <i>spo0A12 <math>\Delta</math>204 <math>\Delta</math>abrB6 trpC2 phe-1</i>   | J. Hoch; 42                                  |
| JH12604        | $\Delta$ <i>amyE::<math>\Phi</math>(abrB-lacZ) cat trpC2 phe-1</i>   | 40   |
| JH12609        | $\Delta$ <i>amyE::<math>\Phi</math>(abrB-lacZ) cat spo0A12 <math>\Delta</math>204 <math>\Delta</math>abrB4 trpC2 phe-1</i> | 40   |
| JH12661        | $\Delta$ <i>amyE::<math>\Phi</math>(abrB-lacZ) cat spo0A12 <math>\Delta</math>204 trpC2 phe-1</i>                          | 40   |
| JH12665        | $\Delta$ <i>amyE::<math>\Phi</math>(abrB-lacZ) cat <math>\Delta</math>abrB4 trpC2 phe-1</i>                                | 40   |
| JH12602        | $\Phi$ ( <i>abrB-lacZ</i> )5139 <i>cat trpC2 phe-1</i>   | J. Hoch; 31                                  |
| JH12560        | $\Phi$ ( <i>abrB-lacZ</i> )5139 <i>cat spo0A12 trpC2 phe-1</i>   | J. Hoch; 31                                  |
| JH12563        | $\Phi$ ( <i>abrB-lacZ</i> )5139 <i>cat spo0A12 <math>\Delta</math>abrB15 trpC2 phe-1</i>                                   | J. Hoch; 31                                  |
| JH12364        | $\Phi$ ( <i>abrB15-lacZ</i> )5139 <i>cat spo0A12 trpC2 phe-1</i>   | J. Hoch; 31                                  |
| SF520          | $\Delta$ <i>amyE::lacZ cat trpC2</i>   | 168 $\times$ pSF1; 45                        |
| SF521          | $\Delta$ <i>amyE::<math>\Phi</math>(hut-lacZ)605 cat trpC2</i>   | 168 $\times$ pHUT605; 45                     |
| SF522          | $\Delta$ <i>amyE::<math>\Phi</math>(hut-lacZ)606 cat trpC2</i>   | 168 $\times$ pHUT606; 45                     |
| SF523          | $\Delta$ <i>amyE::lacZ cat trpC2 phe-1</i>   | JH642 $\times$ SF520 DNA                     |
| SF524          | $\Delta$ <i>amyE::<math>\Phi</math>(hut-lacZ)605 cat trpC2 phe-1</i>   | JH642 $\times$ SF521 DNA                     |
| SF525          | $\Delta$ <i>amyE::<math>\Phi</math>(hut-lacZ)606 cat trpC2 phe-1</i>   | JH642 $\times$ SF522 DNA                     |
| SF526          | $\Delta$ <i>amyE::<math>\Phi</math>(hut-lacZ)605 cat spo0A12 trpC2 phe-1</i>   | JH642 $\times$ SF521 and JH646 DNAs          |
| SF527          | $\Delta$ <i>amyE::<math>\Phi</math>(hut-lacZ)606 cat spo0A12 trpC2 phe-1</i>   | JH642 $\times$ SF522 and JH646 DNAs          |
| SF528          | $\Delta$ <i>amyE::<math>\Phi</math>(hut-lacZ)605 cat spo0A12 <math>\Delta</math>abrB::neo trpC2 phe-1</i>                  | SF524 $\times$ SF514 DNA                     |
| SF529          | $\Delta$ <i>amyE::<math>\Phi</math>(hut-lacZ)606 cat spo0A12 <math>\Delta</math>abrB::neo trpC2 phe-1</i>                  | SF525 $\times$ SF514 DNA                     |
| SF1685         | <i>trpC2 hutU::Tn917-lacZ</i>  | 3  |
| SF1685R        | <i>trpC2 hutU::Tn917-lacZ hutO<sub>CR2</sub>4</i>  | 3, 45  |
| SF6425         | <i>trpC2 phe-1 hutU::Tn917-lacZ</i>  | JH642 $\times$ SF1685 DNA                    |
| SF6425R        | <i>trpC2 phe-1 hutO<sub>CR2</sub>4 hutU::Tn917-lacZ</i>  | JH642 $\times$ SF1685R DNA                   |
| SF6465         | <i>trpC2 phe-1 spo0A12 hutU::Tn917-lacZ</i>  | JH642 $\times$ JH646 and SF1685 DNAs         |
| SF6465R        | <i>trpC2 phe-1 spo0A12 hutU::Tn917-lacZ hutO<sub>CR2</sub>4</i>  | JH642 $\times$ JH646 and SF1685R DNAs        |

<sup>a</sup> Genotype symbols are those of Anagnostopoulos et al. (1), except that *hutO<sub>CR2</sub>4* replaces *hutR4* (9, 45).

directly alters *hut* expression by binding to the *hutO<sub>CR2</sub>* site and thereby interfering with catabolite repression of *hut* transcription.

## MATERIALS AND METHODS

**Bacterial strains.** The bacterial strains used are listed in Table 1. *B. subtilis* chromosomal DNA for transformations and competent cells of *B. subtilis* were prepared as previously described (37). Because *spo0A* mutants are deficient in transformation, *spo0A* mutant strains containing the *hutU::Tn917-lacZ*,  $\Delta$ *abrB::cat*, *abrB::neo*,  $\Delta$ *hpr::cat* gene disruptions and the  $\Delta$ *amyE:: $\Phi$ (hut-lacZ)605 cat* and  $\Delta$ *amyE:: $\Phi$ (hut-lacZ)606 cat* gene fusions were constructed by transforming competent JH642 cells with equal amounts of chromosomal DNA isolated from strain JH646 (*spo0A12*) and from strains containing the appropriate gene construct. Transformants were selected by

using the antibiotic resistance gene linked to the gene construct and then screened for the *spo0A* allele by streaking on Difco sporulation medium (DSM) plates, where *spo0A* mutant strains form translucent colonies. The protease and antibiotic production phenotype of all of the *spo0A* and *abrB* mutant strains used in this work was verified as previously described (42).

**Cell growth and media.** The methods used for bacterial cultivation have been previously described (2, 3). DSM (37), a nutrient sporulation medium, and the morpholinepropanesulfonic acid (MOPS) minimal medium of Neidhardt et al. (25) have been previously described. Glucose was added at 0.5% to MOPS minimal medium. All other carbon and nitrogen sources, except where otherwise noted, were added at 0.2% to this minimal medium. Solutions of L-histidine were freshly prepared, filter sterilized, and added at 0.1% to MOPS mini-

mal medium and at 0.01% to DSM (DSM-His) to induce the histidine-degradative enzymes.

**Enzyme assays.** Extracts for enzyme assays were prepared from cells grown to the mid-log growth phase (70 to 90 Klett units) as previously described (2). Protein concentration was determined by the method of Lowry et al. (20) with bovine serum albumin as the standard.

Histidase,  $\beta$ -galactosidase, inositol dehydrogenase, and  $\alpha$ -glucosidase were assayed in crude cell extracts as described previously (2). One unit of histidase activity produced 1 nmol of urocanic acid per min. One unit of  $\beta$ -galactosidase activity produced 1 nmol of *o*-nitrophenol per min.  $\beta$ -Galactosidase activity was always corrected for the endogenous  $\beta$ -galactosidase specific activity present in SF523 cells (0.04 in glucose-grown cells and 0.4 in arabinose-grown cells). One unit of inositol dehydrogenase caused the reduction of 1 nmol of NAD<sup>+</sup> per min. One unit of  $\alpha$ -glucosidase activity caused an increase in  $A_{420}$  of 0.001/min.

Aconitase was assayed as previously described (2), in cell extracts prepared immediately after the cultures were harvested. One unit of aconitase activity produced 1 nmol of *cis*-aconitate per min. A modified version of the method of Boylan et al. (5) for assaying arabinose isomerase was used. Harvested cells were washed and lysed in 100 mM Tris (pH 7.5) buffer. Under these assay conditions, 1  $\mu$ mol of ribulose gave an  $A_{540}$  of 0.6. One unit of arabinose isomerase activity produced 1  $\mu$ mol of ribulose per min.  $\beta$ -Xylosidase activity was determined by monitoring the production of *p*-nitrophenol from *p*-nitrophenyl- $\beta$ -D-xylopyranoside (Sigma) in cell extracts prepared with Z buffer (23). The reaction mixtures contained 0.5 ml of *p*-nitrophenyl- $\beta$ -D-xylopyranoside (2 mg/ml in 0.1 M potassium phosphate buffer [pH 6.8]) and enough Z buffer and cell extract to bring the volume to 1 ml. The increase in  $A_{410}$  at 25°C was monitored with a Beckman recording spectrophotometer. One unit of  $\beta$ -xylosidase activity produces an increase in optical density at 410 nm of 0.01/min/ml of reaction mixture.

Cell extracts for gluconate kinase and gluconate-6-phosphate dehydrogenase were prepared by a modification of the method described by Fujita and Freese (16). The lysis buffer was supplemented with 50  $\mu$ g of DNase per ml. Gluconate kinase activity was measured as gluconate-dependent production of gluconate-6-phosphate by using endogenous gluconate-6-phosphate dehydrogenase to couple gluconate-6-phosphate production to NADPH formation. To verify that all of the cell extracts contained similar levels of gluconate-6-phosphate dehydrogenase, the level of this enzyme was always measured in extracts used for gluconate kinase assays. The reaction conditions used for the gluconate kinase assays were as previously described (16), except that no exogenous gluconate-6-phosphate dehydrogenase was included in the reaction mixture. One unit of gluconate kinase activity produces 1 nmol of NADPH per min. Gluconate-6-phosphate dehydrogenase activity was measured as previously described (32). One unit of gluconate-6-phosphate dehydrogenase activity produces 1 nmol of NADPH per min.

Lactate dehydrogenase activity was determined by using a modification of the assay described previously (46). Cell extracts were prepared in 0.05 M potassium phosphate buffer (pH 7.5) containing 150 mM NaCl, 150  $\mu$ g of lysozyme per ml, and 50  $\mu$ g of DNase per ml. Preparations were centrifuged for 40 min in an Eppendorf Microfuge at 14,000 rpm and 4°C, and the cleared supernatant was assayed for lactate dehydrogenase activity immediately. The increase in  $A_{340}$  at 30°C was monitored with a Beckman recording spectrophotometer. One unit of lactate dehydrogenase activity caused the oxidation of 1 nmol of NADH per min.

A modification of the assay described by Kane et al. (19) was used to determine glutamate dehydrogenase levels. Harvested cells were washed twice with buffer A (0.04 M potassium phosphate buffer [pH 7.5] containing 30% glycerol and 12 mM  $\beta$ -mercaptoethanol). Cell extracts were prepared immediately following harvesting with buffer A supplemented with 5 mM 2-ketoglutarate. The reaction mixture contained 100 mM Tris-HCl (pH 7.25), 10 mM 2-ketoglutarate, 0.1 mM NADH, and 50 mM NH<sub>2</sub>SO<sub>4</sub>. The decrease in  $A_{340}$  at 37°C was monitored with a Beckman recording spectrophotometer. One unit of glutamate dehydrogenase activity caused the oxidation of 1 nmol of NADH per min.

**Plasmids and DNase I footprinting experiments.** Plasmid pHUT484 was constructed by cloning the *MunI*-*NspI* DNA fragment containing the *hutO*<sub>CR2</sub> site (see Fig. 2) into pMTL23P (8). Plasmid pHUT485 is identical to pHUT484, except that it contains the *hutO*<sub>CR2</sub>4 mutation.

DNase I footprinting experiments were performed with plasmids pHUT484 (wild type) and pHUT485 (*hutO*<sub>CR2</sub>4). The *hut* DNA inserts from these plasmids were excised by using the *Bam*HI and *Stu*I restriction sites in the plasmid polylinker region and end labelled at the *Bam*HI restriction site (which is adjacent to the *MunI* site of the *hut* DNA insert) by using the Klenow enzyme (Bethesda Research Laboratories, Inc.) and [ $\alpha$ -<sup>32</sup>P]dATP (Amersham). DNase I footprinting reactions were performed as previously described (41), except that the final reaction volume was 15  $\mu$ l. The labelled fragments were also subjected to Maxam-Gilbert A+G and C+T sequencing reactions (22) to generate a reference ladder.

## RESULTS

***hut* expression in stationary-phase cultures of wild-type and mutant strains.** During growth in nutrient sporulation medium, the level of histidase, the first enzyme of the histidine-degradative pathway, increased 40- to 200-fold at the onset of the stationary growth phase compared with the level observed during early-exponential-phase growth (Fig. 1A; 3). In strain JH646 (*spo0A12*), histidase specific activity increased 20 to 30 min earlier and reached a higher level than in strain JH642 (wild-type) cultures (Fig. 1A and data not shown). In contrast, the wild-type pattern of histidase expression was observed in SF511 (*spo0A12*  $\Delta$ *abrB::cat*) cultures (Fig. 1A and data not shown). This suggests that the increased levels of histidase observed in the *spo0A* mutant cultures is due to increased levels of AbrB.

When wild-type cells were grown in nutrient sporulation medium lacking Mn<sup>2+</sup>, histidase expression increased only slightly during stationary-phase growth (Fig. 1B). It has been demonstrated previously that this reduction in histidase synthesis is due, in part, to carbon catabolite repression (3, 43). When strain JH646 (*spo0A12*) was grown in nutrient sporulation medium lacking Mn<sup>2+</sup>, histidase expression during stationary-phase growth became derepressed to levels that were 5- to 10-fold higher than those seen in strains JH642 (wild type) and SF511 (*spo0A12*  $\Delta$ *abrB::cat*) (Fig. 1B). This suggests that the effect of the *spo0A* mutation is to partially relieve catabolite repression of *hut* expression and that the AbrB protein is required for this relief of repression.

***hut* expression in wild-type and mutant strains during vegetative growth.** Boylan et al. (5) previously observed that histidase levels are higher in *spo0* mutant cultures than in wild-type cultures during the logarithmic growth phase in minimal media containing slowly metabolized carbon sources. In confirmation of those results, histidase levels in arabinose-grown cultures harvested during mid-exponential-phase

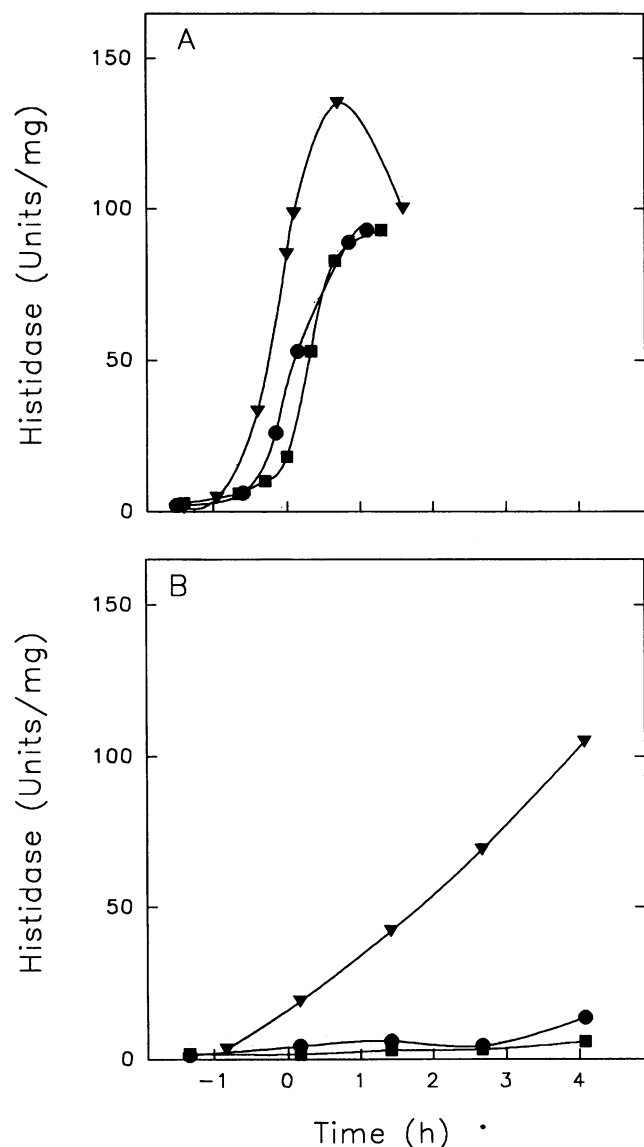


FIG. 1. Histidase levels in wild-type and mutant strains during growth in nutrient sporulation medium. Samples were removed periodically, and histidase activity was determined in extracts of JH462 (wild-type) (●), JH646 (*spo0A12*) (▼), and SF511 (*spo0A12 ΔabrB::cat*) (■) cultures. Cultures were grown in either DSM-His (A) or a version of DSM-His which lacked  $MnCl_2$  (B). The data presented are from a typical experiment.  $T_0$  corresponds to the end of the exponential growth phase.

growth were fivefold higher in JH646 (*spo0A12*) and JH703 (*spo0AΔ204*) extracts than in JH642 (wild-type) extracts (Table 2). However, when the growth medium contained glucose as the carbon source, histidase specific activities in wild-type and *spo0A* mutant cultures were similar (Table 2).

Strains containing *spo0A abrB* mutations were previously separated into two classes on the basis of antibiotic production and genetic analysis (31, 42). The first class of *abrB* mutations, represented by strains SF514, SF511, R15-8, R15-13, JH703abrB1, JH703abrB2, JH703abrB4, and JH703abrB5, produce antibiotic to the same extent as wild-type strains and contain mutations that lie within the *abrB* structural gene. In

arabinose-grown cultures of these *spo0A abrB* double mutants, histidase levels were similar to or slightly lower than that observed in JH642 (wild-type) cultures (Table 2). Histidase levels in arabinose-grown cultures of wild-type strains containing *abrB* gene disruptions or the *abrB4* mutation were also similar to those seen in *spo0A* mutant strains (Table 2).

The second class of *spo0A abrB* mutant strains (JH646MS, R15-9, R15-12, JH703abrB3, and JH703abrB6) is deficient in antibiotic production and contains mutations that lie upstream of the *abrB* coding sequence (31, 42). Strains JH646MS, R15-9, JH703abrB3, and JH703abrB6 all contain the same nucleotide lesion in the *abrB* promoter region. Histidase levels in arabinose-grown cultures of this second group of *spo0A abrB* mutant strains were up to twofold higher than that seen in JH642 (wild-type) cultures (Table 2).

In glucose-grown cultures, histidase levels in extracts of all of the *spo0A abrB* mutant strains were about 1.5- to 3.5-fold lower than that seen in JH642 (wild-type) extracts (Table 2). Similar results were obtained in glucose-grown cultures of strains containing only *abrB* mutations (Table 2). This suggests that catabolite repression of *hut* expression in glucose-grown cultures is more severe in *abrB* mutant strains than in wild-type strains.

Since transcription of the *hpr* gene is positively regulated by the AbrB protein (18, 30, 39), it was necessary to determine whether the altered *hut* expression observed in *spo0A* mutant cultures was mediated by Hpr. Similar levels of histidase were present in extracts of strains SF515 (*spo0A12 Δhpr*) and JH646 (*spo0A12*) grown in arabinose-minimal medium (Table 2). This indicates that the AbrB protein, but not the Hpr protein, is required for the altered *hut* expression observed in *spo0A* mutant cultures grown in minimal medium containing arabinose as the carbon source.

***abrB* expression during vegetative growth.** Transcription of the *abrB* gene is subject to negative autoregulation and repression by the Spo0A protein during growth in nutrient sporulation medium (31, 40). The regulation of *abrB* expression in cultures during mid-exponential-phase growth in minimal media was examined by using an *abrB-lacZ* transcriptional fusion integrated at the *amyE* locus (40).  $\beta$ -Galactosidase levels were four- to fivefold higher in strain JH12661 (*spo0AΔ204*) and JH12665 (*abrB4*) cultures than in strain JH12604 (wild-type) cultures (Table 3). The *abrB4* mutation lies within the *abrB* coding region. The highest level of  $\beta$ -galactosidase expression was observed in strain JH12609 (*spo0AΔ204 abrB4*) cultures (Table 3). These results indicate that the relative levels of *abrB* transcription present in the wild-type and mutant logarithmic-phase cultures in minimal medium are similar to those previously observed in cultures growing exponentially in nutrient sporulation medium (40). *abrB* transcription is not subject to regulation by carbon or nitrogen availability during mid-exponential-phase growth. Similar levels of  $\beta$ -galactosidase were present in wild-type cultures grown in minimal medium containing glucose-glutamate- $NH_4^+$ , arabinose-glutamate- $NH_4^+$ , or glucose-glutamate as carbon and nitrogen sources (Table 3 and data not shown). Comparable results were obtained when  $\beta$ -galactosidase expression was examined in strains JH12661 (*spo0AΔ204*), JH12665 (*abrB4*), and JH12609 (*spo0AΔ204 abrB4*) during mid-exponential-phase growth in medium containing these carbon and nitrogen sources (Table 3 and data not shown).

When JH12661 (*spo0AΔ204*) cultures were grown in minimal medium containing arabinose as the carbon source, a direct correlation between the levels of *abrB* transcription and histidase expression was observed. The levels of both  $\beta$ -galactosidase and histidase were 4.5- to 5-fold higher in extracts of

TABLE 2. Histidase levels in wild-type and mutant strains

| Strain                 | Relevant genotype         | Antibiotic production <sup>a</sup> | Histidase sp act (U/mg of protein) <sup>b</sup> on: |                          |
|------------------------|---------------------------|------------------------------------|---|--------------------------|
|                        |                           |                                    | Glucose <sup>c</sup>                                | L-Arabinose <sup>c</sup> |
| JH642                  | Wild type                 | +                                  | 11 ± 1  | 48 ± 3                   |
| SF513                  | $\Delta$ <i>abrB::cat</i> | +                                  | 4 ± 0.2   | 36 ± 2                   |
| JH642 <i>abrB::neo</i> | <i>abrB::neo</i>          | +                                  | 5 ± 1   | 31 ± 2                   |
| JH12575                | <i>abrB::Tn917</i>        | +                                  | 3 ± 0.1   | 31 ± 3                   |
| JH12663                | <i>abrB4</i>              | +                                  | 8 ± 1   | 39 ± 2                   |
| JH646                  | <i>spo0A12</i>            | —                                  | 8 ± 1   | 250 ± 10                 |
| JH703                  | <i>spo0AΔ204</i>          | —                                  | 10 ± 0.5  | 257 ± 12                 |
| SF514                  | <i>spo0A12 abrB::neo</i>  | +                                  | 6 ± 0.1   | 39 ± 1                   |
| SF511                  | <i>spo0A12 ΔabrB::cat</i> | +                                  | 5 ± 0.2   | 38 ± 8                   |
| R15-8                  | <i>spo0A12 abrB20</i>     | +                                  | 3 ± 0.5   | 38 ± 7                   |
| R15-13                 | <i>spo0A12 abrB23</i>     | +                                  | 5 ± 0.2   | 27 ± 2                   |
| JH703 <i>abrB1</i>     | <i>spo0AΔ204 abrB1</i>    | +                                  | 3 ± 0.2   | 45 ± 2                   |
| JH703 <i>abrB2</i>     | <i>spo0AΔ204 abrB2</i>    | +                                  | 3 ± 0.3   | 36 ± 3                   |
| JH703 <i>abrB4</i>     | <i>spo0AΔ204 abrB4</i>    | +                                  | 4 ± 0.5   | 45 ± 5                   |
| JH703 <i>abrB5</i>     | <i>spo0AΔ204 abrB5</i>    | +                                  | 4 ± 0.2   | 45 ± 2                   |
| JH646MS                | <i>spo0A12 abrB15</i>     | ±                                  | 3 ± 0.3   | 111 ± 10                 |
| R15-9                  | <i>spo0A12 abrB21</i>     | —                                  | 6 ± 0.4   | 82 ± 7                   |
| R15-12                 | <i>spo0A12 abrB22</i>     | ±                                  | 7 ± 0.1   | 83 ± 1                   |
| JH703 <i>abrB3</i>     | <i>spo0AΔ204 abrB3</i>    | ±                                  | 5 ± 0.5   | 95 ± 5                   |
| JH703 <i>abrB6</i>     | <i>spo0AΔ204 abrB6</i>    | ±                                  | 7 ± 0.1   | 58 ± 5                   |
| SF515                  | <i>spo0A12 Δhpr::cat</i>  | —                                  | 13 ± 1  | 245 ± 10                 |

<sup>a</sup> Symbols indicating halo width around isolated colonies of test organisms in a soft agar overlay containing JH646 as the indicator strain (42): —, no zone of clearing was observed; ±, a 0- to 2-mm zone of clearing was observed; +, the zone of clearing was >2 mm.

<sup>b</sup> Averages of three to five determinations ± the standard errors are shown.

<sup>c</sup> Cells were grown in MOPS minimal medium containing the indicated carbon sources, 0.2% NH<sub>4</sub>Cl and 0.2% glutamate as the nitrogen sources, and 0.1% histidine to induce the *hut* operon.

arabinose-grown JH12661 (*spo0AΔ204*) cultures than in JH12604 (wild-type) extracts (Table 3). Although *abrB* transcription was also derepressed in glucose-grown cultures of JH12661 (*spo0AΔ204*) compared with JH12604 (wild-type) cultures, similar histidase levels were present in both cultures (Table 3).

The *abrB15* mutation lies within the *abrB* promoter region and causes reduced *abrB* transcription (31). The levels of *abrB* transcription and histidase expression were determined in *spo0A* mutants containing the *abrB15* mutation to determine whether histidase synthesis in these mutant strains could be correlated with reduced *abrB* transcription. An *abrB-lacZ* transcriptional fusion integrated at the *abrB* locus was used in these experiments (31). When cultures were grown in minimal

medium containing arabinose as the carbon source, the levels of both histidase and β-galactosidase were 4- to 4.5-fold higher in JH12560 (*spo0A12*) extracts than in JH12602 (wild-type) extracts (Table 4). However, when the *abrB-lacZ* fusion contained the *abrB15* allele, β-galactosidase levels increased only 1.7-fold in JH12564 (*spo0A12*) arabinose-grown cultures compared with JH12602 (wild-type) cultures (Table 4). Since histidase levels in arabinose-grown cultures of JH12563 (*spo0A12 abrB15*) were 1.8-fold higher than in JH12602 (wild-type) cultures (Table 4), the levels of *abrB* transcription and histidase expression derepress to the same extent during mid-exponential-phase growth with arabinose as the carbon source.

***hut* expression in wild-type and mutant strains grown in various media.** To identify the nutrient conditions under which AbrB-dependent elevation of histidase synthesis occurs in *spo0A* mutant cells, histidase activity was measured in extracts of wild-type and mutant strains grown in minimal medium containing various carbon and nitrogen sources and harvested during mid-exponential-phase growth. AbrB-dependent activation of *hut* expression in JH646 (*spo0A12*) cultures was observed only when the growth medium contained a carbon source which resulted in reduced growth rates compared with that obtained with glucose, but some poor carbon sources, e.g., trehalose and inositol, did not support elevated histidase production (Table 5). The highest level of histidase derepression occurred in JH646 cultures grown with arabinose as the carbon source (Table 5). Unlike *B. subtilis* 168 and SMY, no growth of strain JH642 was observed in minimal media containing citrate and glutamine as carbon and nitrogen sources (14). AbrB-dependent activation of *hut* expression in *spo0A* mutant cultures appears to be specific to carbon-limited growth, because no elevation in histidase expression was observed in nitrogen-limited *spo0A* mutant cultures grown with glutamate as the sole nitrogen source (Table 5).

TABLE 3. Histidase and β-galactosidase levels in wild-type and mutant strains containing an *amyE::abrB-lacZ* fusion

| Strain  | Relevant genotype <sup>a</sup> | Carbon source <sup>b</sup> | Sp act (U/mg of protein) <sup>c</sup> |           |
|---------|--------------------------------|----------------------------|---------------------------------------|-----------|
|         |                                |                            | β-Galactosidase                       | Histidase |
| JH12604 | Wild type                      | Glucose                    | 62 ± 10                               | 9 ± 1     |
|         |                                | Arabinose                  | 72 ± 10                               | 55 ± 4    |
| JH12661 | <i>spo0AΔ204</i>               | Glucose                    | 277 ± 13                              | 6 ± 2     |
|         |                                | Arabinose                  | 322 ± 8                               | 268 ± 3   |
| JH12609 | <i>spo0AΔ204 abrB4</i>         | Glucose                    | 746 ± 52                              | 4 ± 0.5   |
|         |                                | Arabinose                  | 804 ± 104                             | 43 ± 1    |
| JH12665 | <i>abrB4</i>                   | Glucose                    | 242 ± 5                               | 5 ± 0.1   |
|         |                                | Arabinose                  | 298 ± 41                              | 36 ± 3    |

<sup>a</sup> All strains contain an *abrB-lacZ* transcriptional fusion integrated as a single copy at the chromosomal *amyE* locus (40).

<sup>b</sup> See Table 2, footnote c.

<sup>c</sup> See Table 2, footnote b.

TABLE 4. Histidase and  $\beta$ -galactosidase levels in strains containing an *abrB-lacZ* transcriptional fusion

| Strain  | Relevant genotype     | <i>abrB-lacZ</i> fusion <sup>a</sup> | Carbon source <sup>b</sup> | Sp act (U/mg of protein) <sup>c</sup> |              |
|---------|-----------------------|--------------------------------------|----------------------------|---------------------------------------|--------------|
|         |                       |                                      |                            | $\beta$ -Galactosidase                | Histidase    |
| JH12602 | Wild type             | <i>abrB-lacZ</i>                     | Glucose                    | 282 $\pm$ 9                           | 7 $\pm$ 0.5  |
|         |                       |                                      | Arabinose                  | 314 $\pm$ 9                           | 55 $\pm$ 4   |
| JH12560 | <i>spo0A12</i>        | <i>abrB-lacZ</i>                     | Glucose                    | 1,061 $\pm$ 35                        | 7 $\pm$ 1    |
|         |                       |                                      | Arabinose                  | 1,336 $\pm$ 131                       | 250 $\pm$ 33 |
| JH12564 | <i>spo0A12</i>        | <i>abrB15-lacZ</i>                   | Glucose                    | 497 $\pm$ 20                          | 10 $\pm$ 1   |
|         |                       |                                      | Arabinose                  | 518 $\pm$ 37                          | 321 $\pm$ 24 |
| JH12563 | <i>spo0A12 abrB15</i> | <i>abrB-lacZ</i>                     | Glucose                    | 1,060 $\pm$ 26                        | 5 $\pm$ 1    |
|         |                       |                                      | Arabinose                  | 1,257 $\pm$ 15                        | 97 $\pm$ 1   |

<sup>a</sup> All strains contain an *abrB-lacZ* fusion at the chromosomal *abrB* locus (31). Strains JH12564 and JH12563 were constructed by integrating plasmid pJM5139 (*abrB-lacZ cat*) into strain JH646MS (*abrB15*) by homologous recombination (single crossover). In strain JH12564, the plasmid is integrated so that the *abrB15* mutation lies in the *abrB-lacZ* fusion, while in strain JH12563, the *abrB15* mutation lies within the *abrB* gene.

<sup>b</sup> See Table 2, footnote c.

<sup>c</sup> See Table 3, footnote b.

***hut-lacZ* expression in wild-type and mutant strains.** Because AbrB-dependent activation of *hut* expression occurs only during carbon-limited growth, the AbrB protein may interfere with regulation of the *hut* operon by catabolite repression. Two *cis*-acting sites have been shown to be involved in catabolite repression of *hut* expression (Fig. 2; 27, 45). The *hutO*<sub>CR1</sub> site lies immediately downstream of the *hut* promoter and only weakly regulates *hut* expression. The *hutO*<sub>CR2</sub> site is located downstream of the *hut* transcriptional start site within the *hutP* gene (Fig. 2) and is required for wild-type levels of *hut* regulation in response to carbon availability.

To determine whether the *hutO*<sub>CR2</sub> site is involved in the AbrB-dependent activation of *hut* expression observed in *spo0A* mutants during mid-exponential-phase growth, expression of the *hut-lacZ* 605 and *hut-lacZ* 606 fusions was examined in wild-type and mutant strains. The *hut* DNA fragment in the *hut-lacZ* 605 fusion extends to the *MunI* restriction site which lies immediately upstream of the *hutO*<sub>CR2</sub> site, while the *hut-lacZ* 606 fusion extends beyond and includes *hutO*<sub>CR2</sub> (Fig. 2; 45).

$\beta$ -Galactosidase levels from the *hut-lacZ* 605 fusion were

similar in extracts of SF524 (wild-type) and SF526 (*spo0A12*) cultures grown with either glucose or arabinose as the carbon source (Table 6). This indicates that the site required for AbrB-dependent activation of *hut* expression lies downstream of the *MunI* restriction site in the *hutP* gene. Since the levels of  $\beta$ -galactosidase from the *hut-lacZ* 606 fusion were fivefold higher in extracts of arabinose-grown SF527 (*spo0A12*) cultures than in SF525 (wild-type) or SF529 (*spo0A12 abrB::neo*) extracts (Table 6), AbrB-dependent activation of *hut* expression in *spo0A* mutants requires the *hutO*<sub>CR2</sub> site.  $\beta$ -Galactosidase expression from the *hut-lacZ* 606 fusion in glucose-grown cells was over threefold lower in SF529 (*spo0A12 abrB::neo*) cultures than in either SF525 (wild-type) or SF527 (*spo0A12*) cultures (Table 6). The expected pattern of histidase expression was observed in wild-type and mutant strains containing both *hut-lacZ* fusions.

**AbrB binds to the *hutO*<sub>CR2</sub> site in vitro.** To determine whether the observed AbrB-mediated activation of *hut* expression was due to binding of the AbrB protein to either the *hutO*<sub>CR1</sub> or the *hutO*<sub>CR2</sub> site, DNase I footprinting assays were performed. No binding of AbrB to *hut* DNA containing the *hut*

TABLE 5. Histidase levels in wild-type and mutant cells grown in various media

| Medium composition <sup>a</sup> |                               | Strains                  |  |                          |  |  |  |  |  |
|---------------------------------|-------------------------------|--------------------------|--|--------------------------|--|--|--|--|--|
| Carbon source                   | Nitrogen source               | JH642 (wild type)        |  | JH646 ( <i>spo0A12</i> ) |  | SF511 ( <i>spo0A12</i> $\Delta$ <i>abrB::cat</i> ) |  | JH646MS ( <i>spo0A12</i> <i>abrB15</i> ) |  |
|                                 |                               | dt <sup>b</sup><br>(min) | Histidase<br>sp act<br>(U/mg of<br>protein) <sup>c</sup> | dt<br>(min)              | Histidase<br>sp act<br>(U/mg of<br>protein) <sup>c</sup> | dt<br>(min)  | Histidase<br>sp act<br>(U/mg of<br>protein) <sup>c</sup> | dt<br>(min)                              | Histidase<br>sp act<br>(U/mg of<br>protein) <sup>c</sup> |
| Glucose                         | Glutamate, NH <sub>4</sub> Cl | 60                       | 11   | 45                       | 8  | 75   | 5  | 45                                       | 8  |
| Glucose                         | NH <sub>4</sub> Cl            | 85                       | 27   | 60                       | 26   | 140  | 16   | 60                                       | 31   |
| Glucose                         | Glutamate                     | 110                      | 17   | 65                       | 21   | 110  | 8  | ND                                       | ND   |
| Gluconate                       | Glutamate, NH <sub>4</sub> Cl | 70                       | 25   | 50                       | 55   | 75   | 20   | ND                                       | ND   |
| Trehalose                       | Glutamate, NH <sub>4</sub> Cl | 70                       | 18   | 50                       | 14   | 80   | 9  | 50                                       | 13   |
| Inositol                        | Glutamate, NH <sub>4</sub> Cl | 80                       | 26   | 60                       | 35   | 80   | 11   | 60                                       | 21   |
| Lactate                         | Glutamine                     | 85                       | 40   | 70                       | 113  | 230  | 63   | 70                                       | 68   |
| Citrate                         |                               |                          |  |                          |  |  |  |  |  |
| Maltose                         | Glutamate, NH <sub>4</sub> Cl | 95                       | 74   | 60                       | 192  | 95   | 53   | 60                                       | 137  |
| Arabinose                       | Glutamate, NH <sub>4</sub> Cl | 95                       | 45   | 70                       | 263  | 100  | 38   | 75                                       | 119  |

<sup>a</sup> Cells were grown in MOPS minimal medium containing the indicated carbon and nitrogen sources and 0.1% histidine to induce the *hut* operon.

<sup>b</sup> dt, doubling time.

<sup>c</sup> Average of two or three determinations; values did not vary by more than 25%. ND, not determined.

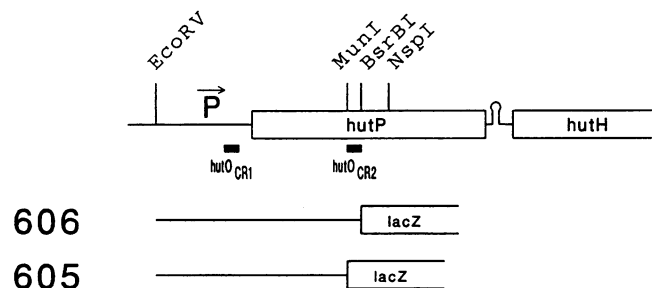


FIG. 2. Structure of the *hut* operon. The restriction and physical map of the *hutPH* genes is taken from reference 28. The locations of the *hutO*<sub>CR1</sub> and *hutO*<sub>CR2</sub> sites (45) are boxed. The *hut* DNA fragments used to construct the *hut-lacZ* 605 and *hut-lacZ* 606 transcriptional fusions (45) are indicated by the solid lines connected to the *lacZ* gene. Abbreviations: P, *hut* promoter region; *hutP*, *hut* regulatory gene; *hutH*, histidase structural gene; *hutO*<sub>CR1</sub> and *hutO*<sub>CR2</sub>, *cis*-acting catabolite repression sites; *lacZ*,  $\beta$ -galactosidase structural gene.

promoter and the *hutO*<sub>CR1</sub> catabolite repression site was detected (data not shown).

The AbrB protein was found to protect a region of approximately 24 bp containing the *hutO*<sub>CR2</sub> operator site from DNase I digestion (Fig. 3A). When the *hut* DNA contained the *hutO*<sub>CR2</sub><sup>4</sup> mutation, AbrB did not bind to this region (Fig. 3B). The *hutO*<sub>CR2</sub><sup>4</sup> mutation lies within the *hutO*<sub>CR2</sub> operator site and causes *hut* expression to be almost completely insensitive to carbon catabolite repression (45). Similar levels of histidase were present in extracts of arabinose-grown cultures of SF6425R (*hutO*<sub>CR2</sub><sup>4</sup>) and SF6465R (*spo0A12 hutO*<sub>CR2</sub><sup>4</sup>) (Table 7). Thus, the AbrB-dependent activation of histidase expression seen in *spo0A* strains requires the wild-type *hutO*<sub>CR2</sub> site.

**Expression of other enzymes regulated by catabolite repression in wild-type and mutant strains.** The expression of other degradative enzymes subject to regulation by catabolite repression was examined in wild-type and mutant cultures during mid-exponential-phase growth to determine whether their expression is subject to modulation by the AbrB protein. The levels of arabinose isomerase, gluconate kinase,  $\alpha$ -glucosidase, and  $\beta$ -xylosidase were 2- to 2.5-fold higher in extracts of JH646 (*spo0A12*) cultures than in JH642 (wild-type) and SF511 (*spo0A12  $\Delta$ abrB::cat*) cultures grown in the media indicated in Table 8. Thus, elevated expression of these enzymes in JH646 (*spo0A12*) cells also requires the AbrB protein. Expression of  $\alpha$ -glucosidase and  $\beta$ -xylosidase is repressed over 100-fold by

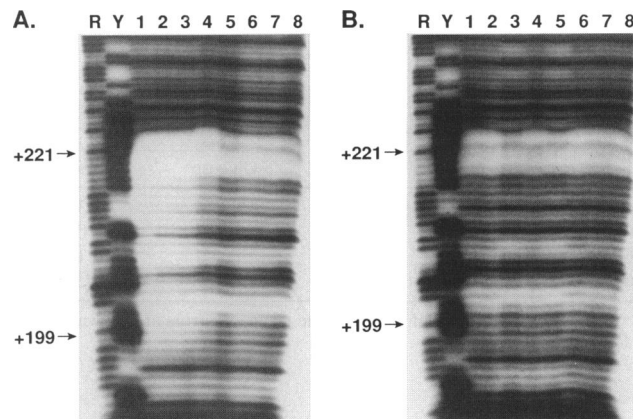


FIG. 3. DNase I protection of the *hutO*<sub>CR2</sub> operator region by the AbrB protein. Results obtained with end-labelled template strands are shown. (A) Binding of the AbrB protein to wild-type *hut* DNA. (B) Binding of the AbrB protein to *hutO*<sub>CR2</sub><sup>4</sup> DNA. AbrB protein concentrations: lanes 1, 30  $\mu$ M; lanes 2, 20  $\mu$ M; lanes 3, 10  $\mu$ M; lanes 4, 3  $\mu$ M; lanes 5, 1.5  $\mu$ M; lanes 6, 0.6  $\mu$ M; lanes 7 and 8, no AbrB protein. The Maxam-Gilbert purine (R) and pyrimidine (Y) sequencing reactions are shown for reference. The numbering system indicates base positions relative to the transcription start site (+1) of the *hut* operon.

glucose in induced wild-type cultures (9, 14, 33), while the induced levels of arabinose isomerase and gluconate kinase are reduced 4- and 10-fold respectively, by growth in the presence of glucose (5, 26, 32, 35). When the expression of these degradative enzymes was examined in induced cultures grown with glucose as the carbon source, all four enzymes were expressed at similar levels in JH642 (wild-type) and JH642 (*spo0A12*) cultures (data not shown).

No AbrB-dependent regulation of inositol dehydrogenase or gluconate dehydrogenase synthesis was detected in JH646 (*spo0A12*) cultures (Table 8 and data not shown). Glucose represses inositol dehydrogenase expression over 100-fold in induced wild-type cultures (2, 9), while no glucose repression of gluconate dehydrogenase synthesis has been reported (32).

Twofold AbrB-dependent activation of aconitase expression was observed in JH646 (*spo0A12*) cultures grown in medium containing lactate, citrate, and glutamine as carbon and nitrogen sources but not when this growth medium also contained glucose (Table 8). The growth rate of SF511 (*spo0A  $\Delta$ abrB::cat*) cultures on medium containing glucose, lactate, and

TABLE 6.  $\beta$ -Galactosidase and histidase levels in wild-type and mutant cells containing *amyE::hut-lacZ* fusions

| Strain <sup>a</sup> | Relevant genotype        | <i>hut-lacZ</i> fusion | Sp act (U/mg of protein) <sup>b</sup> with following carbon source <sup>c</sup> : |             |                        |              |
|---------------------|--------------------------|------------------------|---|-------------|------------------------|--------------|
|                     |                          |                        | Glucose   |             | Arabinose              |              |
|                     |                          |                        | $\beta$ -Galactosidase  | Histidase   | $\beta$ -Galactosidase | Histidase    |
| SF524               | Wild type                | 605                    | 19 $\pm$ 0.5  | 3 $\pm$ 0.2 | 27 $\pm$ 1             | 37 $\pm$ 2   |
| SF526               | <i>spo0A12</i>           | 605                    | 23 $\pm$ 1  | 3 $\pm$ 0.2 | 28 $\pm$ 1             | 192 $\pm$ 17 |
| SF528               | <i>spo0A12 abrB::neo</i> | 605                    | 11 $\pm$ 0.2  | 2 $\pm$ 0.3 | 17 $\pm$ 1             | 26 $\pm$ 1   |
| SF525               | Wild type                | 606                    | 2 $\pm$ 0.1   | 9 $\pm$ 0.1 | 4 $\pm$ 0.1            | 53 $\pm$ 1   |
| SF527               | <i>spo0A12</i>           | 606                    | 2 $\pm$ 0.1   | 7 $\pm$ 0.5 | 22 $\pm$ 2             | 194 $\pm$ 12 |
| SF529               | <i>spo0A12 abrB::neo</i> | 606                    | 0.6 $\pm$ 0.04  | 4 $\pm$ 1   | 3 $\pm$ 0.3            | 37 $\pm$ 2   |

<sup>a</sup> The *hut-lacZ* fusions are integrated as a single copy at the chromosomal *amyE* locus in all of the strains.

<sup>b</sup> Averages of three or four determinations  $\pm$  the standard errors are shown.

<sup>c</sup> See Table 2, footnote c.

TABLE 7. Histidase levels in wild-type and *spo0A* mutant strains containing *hutO*<sub>CR2</sub><sup>Δ</sup> mutations

| Strain  | Relevant genotype                               | Histidase sp act <sup>a</sup> (U/mg of protein) with following carbon source <sup>b</sup> : |           |
|---------|---|---|-----------|
|         |   | Glucose   | Arabinose |
| SF6425  | Wild type                                       | 10 ± 1  | 53 ± 1    |
| SF6425R | <i>hutO</i> <sub>CR2</sub> <sup>Δ</sup>         | 145 ± 14  | 330 ± 14  |
| SF6465  | <i>spo0A12</i>                                  | 9 ± 1   | 221 ± 25  |
| SF6465R | <i>spo0A12 hutO</i> <sub>CR2</sub> <sup>Δ</sup> | 173 ± 2   | 303 ± 30  |

<sup>a</sup> Averages of three determinations ± the standard errors are shown.<sup>b</sup> See Table 2, footnote c.

citrate as carbon sources was significantly slower than that of JH642 (wild-type) cultures (Table 8). This suggests that the presence of high levels of lactate and/or citrate in the growth medium inhibits the growth of the SF511 (*spo0A ΔabrB::cat*) strain.

In *B. subtilis*, glutamate dehydrogenase is involved in glutamate degradation and its synthesis is subject to catabolite repression (19). The levels of glutamate dehydrogenase were fourfold higher in JH642 (wild-type) cells grown in medium containing arabinose as the carbon source than in glucose-grown cultures (data not shown). Unexpectedly, glutamate dehydrogenase activity was not detected in extracts of JH646 (*spo0A12*) cultures grown with either glucose or arabinose as the carbon source because of the high background levels of NADH oxidase activity (data not shown).

Lactate dehydrogenase does not appear to be involved in lactate utilization in *B. subtilis* because the levels of this enzyme were higher in JH642 (wild-type) cultures containing glucose, lactate, and citrate as carbon sources than in JH642 (wild-type) cultures grown with only lactate and citrate as carbon sources (Table 8). However, twofold AbrB-dependent activation of lactate dehydrogenase expression was seen in JH646 (*spo0A12*) cultures grown in minimal medium containing glucose, lactate, and citrate as carbon sources (Table 8). Lactate dehydrogenase expression in *B. subtilis* was previously proposed to be induced by oxidative stress (46). Expression of

several gene products regulated in response to oxidative stress has been proposed to be regulated by the Hpr protein in *B. subtilis* (13). Since the AbrB protein positively activates *hpr* transcription, the twofold AbrB-dependent activation of lactate dehydrogenase expression seen in JH646 (*spo0A12*) glucose-grown cultures may result from Hpr-dependent regulation of lactate dehydrogenase expression.

## DISCUSSION

Several lines of evidence indicate that elevated levels of the AbrB protein are responsible for elevated expression of the *hut* operon in *spo0A* mutant strains during mid-exponential-phase carbon-limited growth. During logarithmic-phase growth in medium containing arabinose as the carbon source, the levels of both *abrB* transcription and *hut* expression are four- to fivefold higher in *spo0A* mutant strains than in wild-type strains. Secondly, both *abrB* transcription and *hut* expression are elevated only 1.8-fold in arabinose-grown cultures of *spo0A abrB15* mutant strains, while no derepression of *hut* expression occurs in *spo0A* mutant strains containing *abrB* null mutations, e.g., *ΔabrB::cat*.

The wild-type *hutO*<sub>CR2</sub> operator site is required for the AbrB-dependent derepression of *hut* expression observed in *spo0A* mutant strains. In DNase I footprinting experiments, the AbrB protein bound to wild-type *hutO*<sub>CR2</sub> operator DNA but not to *hutO*<sub>CR2</sub> operator DNA containing the *hutO*<sub>CR2</sub><sup>Δ</sup> mutation. No sequence motif which serves as the binding site for AbrB has been identified (38). However, there is significant sequence similarity between the *hutO*<sub>CR2</sub> operator site and a proposed AbrB binding determinant. Furthermore, the *hutO*<sub>CR2</sub><sup>Δ</sup> mutation alters a highly conserved cytosine residue within this putative AbrB binding determinant (Fig. 4; 41, 45). The *hut* DNA fragment used for the DNase I footprinting experiments lies between the *MunI* and *NspI* sites in the *hutP* gene (Fig. 2). Since the in vitro AbrB footprint extends up to the *MunI* site, it is possible that the AbrB *hut* binding region extends further upstream in vivo.

Because the *hutO*<sub>CR2</sub> operator site is required for wild-type regulation of the *hut* operon by catabolite repression, AbrB most likely competes with the catabolite repressor protein for

TABLE 8. Levels of various enzymes in wild-type and mutant strains

| Enzyme                  | Growth medium <sup>a</sup> | Strain                |                                       |                          |                                       |                                     |                                       |
|-------------------------|----------------------------|-----------------------|---------------------------------------|--------------------------|---------------------------------------|-------------------------------------|---------------------------------------|
|                         |                            | JH642 (wild type)     |                                       | JH646 ( <i>spo0A12</i> ) |                                       | SF511 ( <i>spo0A12 ΔabrB::cat</i> ) |                                       |
|                         |                            | dt <sup>b</sup> (min) | Sp act (U/mg of protein) <sup>c</sup> | dt (min)                 | Sp act (U/mg of protein) <sup>c</sup> | dt (min)                            | Sp act (U/mg of protein) <sup>c</sup> |
| Arabinose isomerase     | A                          | 95                    | 3 ± 0.05                              | 70                       | 7 ± 0.2                               | 100                                 | 3 ± 0.02                              |
| Aconitase               | B                          | 85                    | 81 ± 21                               | 70                       | 184 ± 3                               | 205                                 | 81 ± 9                                |
| Aconitase               | C                          | 55                    | 11 ± 3                                | 40                       | 15 ± 2                                | 105                                 | 5 ± 0.3                               |
| Gluconate kinase        | D                          | 80                    | 11 ± 1                                | 55                       | 27 ± 1                                | 90                                  | 12 ± 2                                |
| Gluconate dehydrogenase | D                          | 80                    | 77 ± 1                                | 55                       | 65 ± 1                                | 90                                  | 48 ± 6                                |
| α-Glucosidase           | E                          | 110                   | 38 ± 2                                | 50                       | 82 ± 2                                | 115                                 | 33 ± 3                                |
| Inositol dehydrogenase  | F                          | 80                    | 496 ± 17                              | 55                       | 861 ± 31                              | 140                                 | 622 ± 16                              |
| Lactate dehydrogenase   | B                          | 85                    | 3 ± 0.5                               | 70                       | 4 ± 1.5                               | 205                                 | <1                                    |
| Lactate dehydrogenase   | C                          | 55                    | 75 ± 2                                | 40                       | 141 ± 39                              | 105                                 | 29 ± 11                               |
| β-Xylosidase            | G                          | 105                   | 102 ± 3                               | 60                       | 256 ± 5                               | 105                                 | 77 ± 7                                |

<sup>a</sup> Cells were grown in MOPS minimal medium containing the following carbon and nitrogen sources: medium A, 0.2% L-arabinose–0.04% L-glutamate–0.2% NH<sub>4</sub>Cl; medium B, 0.2% L-lactate–0.2% sodium citrate–0.2% L-glutamine; medium C, 0.5% D-glucose–0.2% L-lactate–0.2% sodium citrate–0.2% L-glutamine; medium D, 0.2% D-gluconate–0.04% L-glutamate–0.2% NH<sub>4</sub>Cl–0.2% L-histidine; medium E, 0.2% maltose–0.04% L-glutamate–0.2% NH<sub>4</sub>Cl; medium F, 0.2% *myo*-inositol–0.04% L-glutamate–0.2% NH<sub>4</sub>Cl; medium G, 0.2% D-xylose–0.2% L-aspartate–0.2% L-glutamate–0.2% L-alanine–0.2% NH<sub>4</sub>Cl.

<sup>b</sup> dt, doubling time.<sup>c</sup> Averages of two or three determinations ± the standard errors are shown.





FIG. 4. Nucleotide sequence of *hut* DNA containing the *hutO*<sub>CR2</sub> catabolite repression site. The nucleotides protected by the AbrB protein in DNase I footprinting experiments are indicated below the *hut* DNA sequence. The location and the nucleotide lesion of the *hutO*<sub>CR2</sub>4 mutation (45) are indicated below the *hut* nucleotide sequence. Aligned above the nucleotide sequence of the *hutO*<sub>CR2</sub> region of pHUT484 are the proposed consensus sequences for *B. subtilis* catabolite repression operator sites (44) and the proposed AbrB binding determinant (41) and its complement.

binding to *hutO*<sub>CR2</sub>. AbrB-dependent derepression of *hut* expression is observed only when *spo0A* mutant strains are grown in medium containing carbon sources in which *hut* expression is subject to only partial catabolite repression, e.g., arabinose, maltose, gluconate, or lactate-citrate. We are unable to explain why no alteration in histidase expression occurs when *Spo0A* mutant strains are grown with another poor carbon source, trehalose or inositol. During growth of *spo0A* mutant cultures in medium containing a carbon source which severely represses *hut* expression, e.g., glucose, the elevated levels of AbrB protein are apparently insufficient to compete effectively with the catabolite repressor for binding at the *hutO*<sub>CR2</sub> operator site.

Two different models have been proposed for the mechanism which allows the *hutO*<sub>CR2</sub> site, which lies over 200 nucleotides downstream of the *hut* promoter, to mediate catabolite repression of *hut* expression (45). In the first model, binding of the catabolite repressor protein at the *hutO*<sub>CR2</sub> site acts as a roadblock and terminates transcription, which initiates at the *hut* promoter. According to this model, the AbrB protein bound at the *hutO*<sub>CR2</sub> site would be unable to block transcription elongation by RNA polymerase. In the second model, binding of the catabolite repressor protein to the weak *hutO*<sub>CR1</sub> site is strengthened by cooperative interaction with catabolite repressor protein bound to the downstream *hutO*<sub>CR2</sub> site. In this model, binding of the AbrB protein at the *hutO*<sub>CR2</sub> site would interfere with binding of the catabolite repressor protein at the *hutO*<sub>CR2</sub> site and thus prevent DNA looping between the *hutO*<sub>CR1</sub> and *hutO*<sub>CR2</sub> sites.

Since *hut* expression is still subject to catabolite repression in *abrB* null mutants, AbrB is not solely responsible for regulation of *hut* expression in response to carbon availability. In fact, histidase expression is more repressed in glucose-grown SF511 ( $\Delta$ *abrB::cat*) cultures than in wild-type cultures (Tables 2 and 5). This suggests that absence of the AbrB protein increases the severity of catabolite repression during mid-exponential-phase growth and supports the model in which AbrB binds to the *hutO*<sub>CR2</sub> site in vivo.

The AbrB protein is able to alter the expression of several other enzymes whose expression is subject to catabolite repression. It is unclear whether this AbrB-dependent effect is direct or indirect. Catabolite repression of gluconate kinase (*gnt*) expression is mediated by a downstream operator site with significant similarity to the *hutO*<sub>CR2</sub> site (24). Thus, AbrB might affect the expression of both histidase and gluconate kinase by similar mechanisms. In contrast, catabolite repres-

sion of *hut* and aconitase (*citB*) expression appears to be mediated by different mechanisms. Significant catabolite repression of *citB* expression occurs only in cultures grown in the presence of both glucose and a good source of 2-ketoglutarate (34). Furthermore, no sequence similarity exists between the sites required for catabolite repression of aconitase (*citB*) and of *hut* expression (15). This suggests that the effect of AbrB on aconitase expression is indirect. However, it should be noted that a sequence similar to the proposed AbrB binding determinant is located between positions -58 and -51 in the *citB* promoter region, immediately adjacent to the *citB* catabolite repression site (15, 41).

Interestingly, two- to fourfold overproduction of the AbrB protein significantly increases the growth rates of *B. subtilis* cultures. Both JH646 (*spo0A12*) and JH646MS (*spo0A12 abrB15*) cultures grew faster than did JH642 (wild-type) cultures on all of the growth media examined (Table 5). The *spo0A* mutation is not directly responsible for the increased growth rates, because the growth rate of a *spo0A* mutant strain containing an *abrB* null mutation, e.g., SF511 (*spo0A12*  $\Delta$ *abrB::cat*), was similar to or slower than that of wild-type cultures (Table 5). It is unclear how increased levels of AbrB enhance the growth of *B. subtilis* cultures. In these studies, elevated AbrB levels were shown to alter the expression of genes subject to catabolite repression, but only during carbon-limited growth. Thus, AbrB must modulate expression of other, unidentified gene products in *B. subtilis*. This observation, taken together with the AbrB-dependent alterations in gene expression shown in this work, strongly suggests that AbrB regulates gene expression not only during the transition between the logarithmic and stationary growth phases but also during the logarithmic growth phase.

#### ACKNOWLEDGMENTS

We thank Patricia Rice and Florence Pettengill for excellent technical assistance, J. Hoch for comments on the manuscript, and A. Grossman, J. Hoch, M. Perego, A. L. Sonenshein, and P. Zuber for providing strains. We also thank B. Magasanik for helpful discussions.

This work was supported by U.S. Public Health Service research grants from the National Institutes of Health (AI23168 to S.H.F. and GM46700 to M.A.S.). The Scripps Research Institute has given this communication manuscript number 8252-MEM.

#### REFERENCES

1. Anagnostopoulos, C., P. J. Piggot, and J. A. Hoch. 1993. The genetic map of *Bacillus subtilis*, p. 425-461. In A. L. Sonenshein, J. A. Hoch, and R. Losick (ed.), *Bacillus subtilis* and other gram-positive bacteria: biochemistry, physiology, and molecular genetics. American Society for Microbiology, Washington, D.C.
2. Atkinson, M. R., L. V. Wray, Jr., and S. H. Fisher. 1990. Regulation of histidine and proline degradation enzymes by amino acid availability in *Bacillus subtilis*. J. Bacteriol. 172:4758-4765.
3. Atkinson, M. R., L. V. Wray, Jr., and S. H. Fisher. 1993. Activation of the *Bacillus subtilis* *hut* operon at the onset of stationary growth phase in nutrient sporulation medium results primarily from the relief of amino acid repression of histidine transport. J. Bacteriol. 175:4282-4289.
4. Bisschop, A., L. de Jong, M. E. Lima Costa, and W. N. Konings. 1975. Relation between reduced nicotinamide adenine dinucleotide oxidation and amino acid transport in membrane vesicles from *Bacillus subtilis*. J. Bacteriol. 121:807-813.
5. Boylan, S. A., K. T. Chun, B. A. Edson, and C. W. Price. 1988. Early-blocked sporulation mutations alter expression of enzymes under carbon control in *Bacillus subtilis*. Mol. Gen. Genet. 212: 271-280.
6. Brehm, S. P., S. P. Staal, and J. A. Hoch. 1973. Phenotypes of pleiotropic-negative sporulation mutants of *Bacillus subtilis*. J. Bacteriol. 115:1063-1070.
7. Burbulys, D., K. A. Trach, and J. A. Hoch. 1991. Initiation of

- sporulation in *Bacillus subtilis* is controlled by a multicomponent phosphorelay. *Cell* **64**:545–552.
8. Chambers, S. P., S. E. Prior, D. A. Barstow, and N. P. Minton. 1988. The pMTL *nic*<sup>−</sup> cloning vectors. I. Improved pUC polylinker regions facilitate the use of sonicated DNA for nucleotide sequencing. *Gene* **68**:139–149.
  9. Chasin, L. A., and B. Magasanik. 1968. Induction and repression of the histidine-degrading enzymes of *Bacillus subtilis*. *J. Biol. Chem.* **243**:5165–5178.
  10. Cooney, P. H., P. F. Whiteman, and E. Freese. 1977. Media dependence of commitment in *Bacillus subtilis*. *J. Bacteriol.* **129**:901–907.
  11. Deutscher, M. P., and A. Kornberg. 1968. Biochemical studies of bacterial sporulation and germination. VIII. Patterns of enzyme development during growth and sporulation of *Bacillus subtilis*. *J. Biol. Chem.* **243**:4653–4660.
  12. Dingman, D. W., M. S. Rosenkrantz, and A. L. Sonenshein. 1987. Relationship between aconitase gene expression and sporulation in *Bacillus subtilis*. *J. Bacteriol.* **169**:3068–3075.
  13. Dowds, B. C. A., and J. A. Hoch. 1991. Regulation of the oxidation stress response by the *hpr* gene in *Bacillus subtilis*. *J. Gen. Microbiol.* **137**:1121–1125.
  14. Fisher, S. H. Unpublished data.
  15. Fouet, A., and A. L. Sonenshein. 1990. A target for carbon source-dependent negative regulation of the *citB* promoter of *Bacillus subtilis*. *J. Bacteriol.* **172**:835–844.
  16. Fujita, Y., and E. Freese. 1981. Isolation and properties of a *Bacillus subtilis* mutant unable to produce fructose-bisphosphatase. *J. Bacteriol.* **145**:760–767.
  17. Fürbaß, R., M. Gocht, P. Zuber, and M. A. Marahiel. 1991. Interaction of AbrB, a transcriptional regulator from *Bacillus subtilis* with the promoters of the transition state-activated genes *tycA* and *spo0VG*. *Mol. Gen. Genet.* **225**:347–354.
  18. Kallio, P. T., J. E. Fagelson, J. A. Hoch, and M. A. Strauch. 1991. The transition state regulator Hpr of *Bacillus subtilis* is a DNA-binding protein. *J. Biol. Chem.* **266**:13411–13417.
  19. Kane, J. F., J. Wakim, and R. S. Fischer. 1981. Regulation of glutamate dehydrogenase in *Bacillus subtilis*. *J. Bacteriol.* **148**:1002–1005.
  20. Lowry, O. H., N. J. Rosebrough, A. L. Farr, and R. J. Randall. 1951. Protein measurement with the Folin phenol reagent. *J. Biol. Chem.* **193**:265–275.
  21. Mathiopoulos, C., J. P. Mueller, F. J. Slack, C. G. Murphy, S. Patanker, G. Bukusoglu, and A. L. Sonenshein. 1991. A *Bacillus subtilis* dipeptide transport system expressed early during sporulation. *Mol. Microbiol.* **5**:1903–1913.
  22. Maxam, A. M., and W. Gilbert. 1980. Sequencing end-labeled DNA with base-specific chemical cleavages. *Methods Enzymol.* **65**:499–560.
  23. Miller, J. H. 1972. Experiments in molecular genetics, p. 355. Cold Spring Harbor Laboratory, Cold Spring Harbor, N.Y.
  24. Miwa, Y., and Y. Fujita. 1993. Promoter-independent catabolite repression of the *Bacillus subtilis* *gnt* operon. *J. Biochem.* **113**:665–671.
  25. Neidhardt, F. C., P. L. Bloch, and D. F. Smith. 1974. Culture medium for enterobacteria. *J. Bacteriol.* **119**:736–747.
  26. Nihashi, J.-I., and Y. Fujita. 1984. Catabolite repression of inositol dehydrogenase and gluconate kinase synthesis of *Bacillus subtilis*. *Biochim. Biophys. Acta* **798**:88–95.
  27. Oda, M., T. Katagai, D. Tomura, H. Shoun, T. Hoshino, and K. Furukawa. 1992. Analysis of the transcriptional activity of the *hut* promoter in *Bacillus subtilis* and identification of a *cis*-acting regulatory region associated with catabolite repression downstream from the site of transcription. *Mol. Microbiol.* **6**:2573–2582.
  28. Oda, M., A. Sugishita, and K. Furukawa. 1988. Cloning and nucleotide sequences of histidase and regulatory genes in the *Bacillus subtilis* *hut* operon and positive regulation of the operon. *J. Bacteriol.* **170**:3199–3205.
  29. Ohné, M. 1975. Regulation of the dicarboxylic acid part of the citric acid cycle in *Bacillus subtilis*. *J. Bacteriol.* **122**:224–234.
  30. Perego, M., and J. A. Hoch. 1988. Sequence analysis and regulation of the *hpr* locus, a regulatory gene for protease production and sporulation in *Bacillus subtilis*. *J. Bacteriol.* **170**:2560–2567.
  31. Perego, M., G. B. Spiegelman, and J. A. Hoch. 1988. Structure of the gene for the transition state regulator, *abrB*: regulator synthesis is controlled by the *spo0A* sporulation gene in *Bacillus subtilis*. *Mol. Microbiol.* **2**:689–699.
  32. Reizer, A., J. Deutscher, M. H. Saier, Jr., and J. Reizer. 1991. Analysis of the gluconate (*gnt*) operon of *Bacillus subtilis*. *Mol. Microbiol.* **5**:1081–1089.
  33. Roncero, M. I. G. 1983. Genes controlling xylan utilization by *Bacillus subtilis*. *J. Bacteriol.* **156**:257–263.
  34. Rosenkrantz, M. S., D. W. Dingman, and A. L. Sonenshein. 1985. *Bacillus subtilis* *citB* gene is regulated synergistically by glucose and glutamine. *J. Bacteriol.* **164**:155–164.
  35. Sá-Nogueira, I., H. Paveia, and H. de Lencastre. 1988. Isolation of constitutive mutants for L-arabinose utilization in *Bacillus subtilis*. *J. Bacteriol.* **170**:2855–2857.
  36. Sonenshein, A. L. 1989. Metabolic regulation of sporulation and other stationary-phase phenomena, p. 109–130. In I. Smith, R. A. Slepecky, and P. Setlow (ed.), Regulation of prokaryotic development: structural and functional analysis of bacterial sporulation and germination. American Society for Microbiology, Washington, D.C.
  37. Sonenshein, A. L., B. Cami, J. Brevet, and R. Cote. 1974. Isolation and characterization of rifampin-resistant and streptolydigin-resistant mutants of *Bacillus subtilis* with altered sporulation properties. *J. Bacteriol.* **120**:253–265.
  38. Strauch, M. A. 1993. AbrB, a transition state regulator, p. 757–764. In A. L. Sonenshein, J. A. Hoch, and R. Losick (ed.), *Bacillus subtilis* and other gram-positive bacteria: biochemistry, physiology, and molecular genetics. American Society for Microbiology, Washington, D.C.
  39. Strauch, M. A., and J. A. Hoch. 1993. Transition-state regulators: sentinels of *Bacillus subtilis* post-exponential gene expression. *Mol. Microbiol.* **7**:337–342.
  40. Strauch, M. A., M. Perego, D. Burbulys, and J. A. Hoch. 1989. The transition state transcription regulator AbrB of *Bacillus subtilis* is autoregulated during vegetative growth. *Mol. Microbiol.* **3**:1203–1209.
  41. Strauch, M. A., G. B. Spiegelman, M. Perego, W. C. Johnson, D. Burbulys, and J. A. Hoch. 1989. The transition state transcription regulator *abrB* of *Bacillus subtilis* is a DNA binding protein. *EMBO J.* **8**:1615–1621.
  42. Trowsdale, J., S. M. H. Chen, and J. A. Hoch. 1979. Genetic analysis of phenotypic revertants of *spo0A* mutants in *Bacillus subtilis*: a new cluster of ribosomal genes, p. 131–135. In G. Chambliss and J. C. Vary (ed.), Spores VII. American Society for Microbiology, Washington, D.C.
  43. Vasantha, N., and E. Freese. 1979. The role of manganese in growth and sporulation of *Bacillus subtilis*. *J. Gen. Microbiol.* **112**:329–336.
  44. Weickert, M. J., and G. H. Chambliss. 1990. Site-directed mutagenesis of a catabolite repression operator sequence in *Bacillus subtilis*. *Proc. Natl. Acad. Sci. USA* **87**:6238–6242.
  45. Wray, L. V., Jr., F. K. Pettengill, and S. H. Fisher. 1994. Catabolite repression of the *Bacillus subtilis* *hut* operon requires a *cis*-acting site located downstream of the transcription initiation site. *J. Bacteriol.* **176**:1894–1902.
  46. Yashphe, J., J. A. Hoch, and N. O. Kaplan. 1978. Regulation of lactate dehydrogenase synthesis in *Bacillus subtilis*. *Biochim. Biophys. Acta* **544**:1–7.